

## UWB-BPF WITH APPLICATION BASED TRIPLE NOTCHES AND SUPPRESSED STOPBAND

Abu N. Ghazali<sup>1, \*</sup> and Srikanta Pal<sup>2</sup>

<sup>1</sup>Department of Electronics & Communication Engineering, Birla Institute of Technology, Mesra, Patna Campus 800014, India

<sup>2</sup>Department of Electronics & Communication Engineering, Birla Institute of Technology, Mesra, Ranchi 835215, India

**Abstract**—An ultra-wideband (UWB) bandpass filter (BPF) with application oriented triple notches and simultaneously suppressed stopband is proposed. Implementing complementary split ring resonator (CSR) and novel complementary meandered folded split ring resonators (CMFSRR) shaped defected ground structures (DGS) in the ground of proposed structure generates the triple notch in the UWB passband. The notch positions are functions of CSR/CMFSRR profile dimensions. Stopband is suppressed using the dual attenuation poles generated by the double equilateral-U (DEU) shaped DGS. An approximate lumped equivalent circuit model of the proposed filter is presented. Measured results obtained are in good agreement with the equivalent circuit model and full wave electromagnetic (EM) simulation. The filter is small in size with an overall area of 26.06 mm × 11 mm.

### 1. INTRODUCTION

Recently research on ultra-wideband (UWB) bandpass filters (BPF) with multiple controllable notches within the passband has been carried out to eliminate in-band interferences from various wireless communication services like wireless local area network (WLAN), C and military (X) band, etc. Initial reported design techniques of UWB-BPF mainly focused on realizing satisfactory passband but most of them neglected the problem of in-band interference and/or narrow stopband [1–4]. UWB-BPF which addressed the above shortcomings hence became a necessity [5–8].

---

*Received 15 March 2013, Accepted 15 April 2013, Scheduled 24 April 2013*

\* Corresponding author: Abu Nasar Ghazali (anghazali@gmail.com).

An UWB filter with dual notched band using asymmetric coupling was reported in [5]. Simplified composite right/left-handed resonators based dual notched band UWB filter was reported in [6], while two mushroom type electromagnetic bandgap (EBG) structures generated dual notch bands in [7]. An UWB bandpass filter with triple notched bands using a triple mode stepped impedance resonator is reported in [8]. None of [5–8] reported simultaneously significant extended stopband.

In this letter, we propose an UWB-BPF with triple notched band and simultaneously extended stopband. The original filter is designed; into which complementary square split ring resonator (CSRR) and novel complementary meandered folded split ring resonators (CMFSRR) shaped defected ground structure (DGS) are implemented to generate the triple notches wherein the notch positions are functions of CSRR/CMFSRR profile dimensions. Double equilateral-U (DEU) [9] shaped DGS implemented under input and output feeding lines generate dual flexible attenuation poles whose proper positioning suppress the spurious harmonics and extend the stopband. Also an approximate lumped equivalent circuit model of the proposed structure is developed. Later the filter is fabricated whose performance is compared and verified with the full wave EM and circuit simulation.

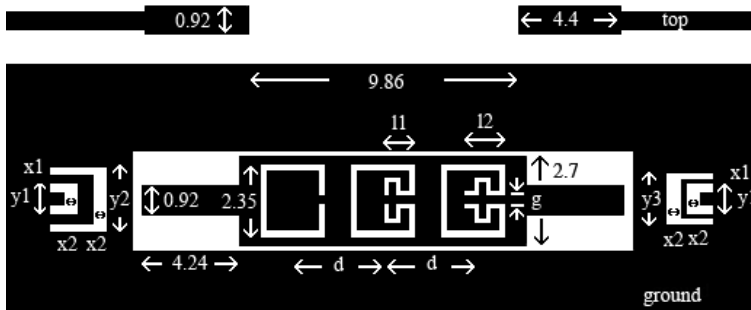


**Figure 1.** The proposed filter. Microstrip lines on the top and the ground plane has CMFSRRs and CSRR etched on the MMR with DEU-DGS under the input and output feeding lines. Dark shade represents conductor and white shade represents etched part, all dimensions in mm.

## 2. UWB FILTER DESIGN

The proposed UWB filter, shown in Fig. 1, is modeled based on the back-to-back microstrip-to-co-planar waveguide (CPW) technology [1] and designed using the commercial, full wave electromagnetic (EM) IE3D software [10]. The ground has multiple mode resonator (MMR) based CPW coupled in broadside fashion to the microstrip lines on the top. Fig. 2(a) depicts the open circuited MMR with wide and narrow arms of impedances  $Z_1$ ,  $Z_2$  and electrical lengths  $2\theta_1$ ,  $\theta_2$ , respectively. This MMR has an equivalent transmission line topology which consists of three cascaded sections as shown in Fig. 2(b). The resonant modes of this MMR are evaluated from its input admittance ( $Y_{in}$ ), at the left end looking into the right [11]:

$$Y_{in} = jY_2 \frac{2(Rz \tan \theta_1 + \tan \theta_2)(Rz - \tan \theta_1 \tan \theta_2)}{Rz(1 - \tan^2 \theta_1)(1 - \tan^2 \theta_2) - 2(1 + Rz^2) \tan \theta_1 \tan \theta_2} \quad (1)$$

For the resonance condition  $Y_{in} = 0$ , and Equation (1) reduces to

$$Rz \tan \theta_1 + \tan \theta_2 = 0 \quad (2)$$

$$Rz - \tan \theta_1 \tan \theta_2 = 0 \quad (3)$$

where  $Rz$  is the ratio of two characteristic impedances, i.e.,  $Rz = Z_2/Z_1 = Y_1/Y_2$ .

Solving (2) and (3) provides us with odd and even mode resonant frequencies, respectively. In general for the MMR, the length ratio of the narrow and wide arms is defined as:

$$x = \frac{\theta_2}{\theta_2 + \theta_1} \quad (4)$$

Replacing (4) in Equations (2) and (3) gives

$$Rz - \tan \theta_1 \tan \frac{x}{1-x} \theta_1 = 0 \quad (5)$$

$$Rz \tan \theta_1 + \tan \frac{x}{1-x} \theta_1 = 0 \quad (6)$$

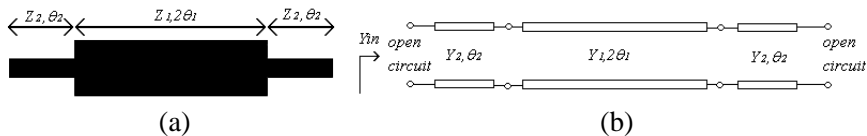


**Figure 2.** (a) Topology of the MMR for the proposed filter.  $Z_1 = 19 \Omega$ ,  $Z_2 = 38 \Omega$  and  $\theta_1 = 117$  degrees,  $\theta_2 = 94$  degrees. (b) Equivalent transmission line circuit of the MMR.

For the proposed UWB filter when  $Rz = 2$  and  $\theta_2 = 0.81\theta_1$  ( $x = 0.447$ ), three resonant frequencies (4.11, 6.8 and 9.15 GHz, respectively) are positioned reasonably close and approximately equi-distant from each other. For the case of weak coupling, Fig. 3 shows the presence of three resonant modes,  $f_1$ ,  $f_2$  and  $f_3$  at 4.1, 6.75 and 9 GHz, respectively, which approximately validates the results obtained analytically. It can be inferred from above that the MMR when properly optimized in profile dimensions simultaneously excites these resonant modes and generates the requisite UWB passband. The optimized modeling of microstrip-to-CPW transition provides a tight capacitive coupling via the dielectric and places the enhanced coupling peak near the central UWB frequency as shown in Fig. 3. This tight electromagnetic coupling of the transition smoothens the passband and reduces the parasitic radiation loss.

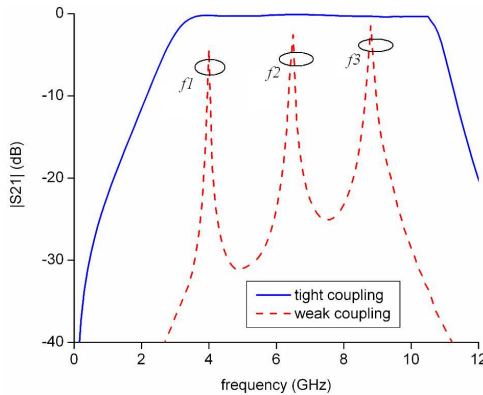


**Figure 3.** Frequency response for weak and tight coupling.

### 2.1. Implementation of Notched Bands

To introduce a single narrow notch, a square shaped CSRR-DGS in the MMR is considered (inset Fig. 4). The notch has resonant frequency,  $f_0 = 1/2\pi\sqrt{LC}$ , where  $L$  and  $C$  are evaluated from [12] as:

$$C = 1/(Z_0 * 4 * \pi * \Delta f_{3\text{dB}}) \text{ and}$$

$$L = 1/(2 * \pi * f)^2 * C$$

Here  $Z_0$  is the characteristic impedance of the transmission line,  $50 \Omega$ , and  $\Delta f_{3\text{dB}}$  is the fractional 3 dB bandwidth of the notch frequency  $f_0$ . The inductance  $L$  is the function of slot lengths while the capacitance  $C$  is the sum of capacitances due to gap between slots and gap at the slots ends.

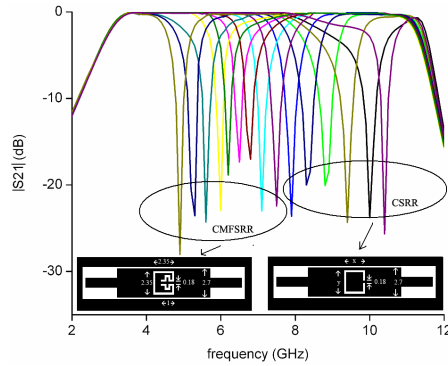


**Figure 4.** CSRR of variable  $y$  ( $= x$ ) represents notches 8 GHz and above. Notches below 8 GHz are for CMFSRR of  $y = x = 2.35$  mm and variable  $l$ .

In the narrow frequency range of  $f_0$ , the effective permeability of the medium becomes negative, and the propagating waves become evanescent waves thereby prohibiting wave propagation, leading to stopband characteristics. To position the notch towards the lower end of UWB passband, gap width,  $g$  ( $= 0.18$  mm), and slot line width ( $0.18$  mm) are kept constant and the length of the thin slot line in the CSRR-DGS layout is varied. The CSRR considered has lower cut-off frequency at 8 GHz for  $y = x = 2.35$  mm, as shown in Fig. 4. To further lower the notch frequency meandered folded slot lines are introduced to the CSRR ( $y = x = 2.35$  mm) to form novel CMFSRR.

Notch with increased bandwidth is obtained by cascading equi-dimensional CMFSRR/CSRR on the MMR. Fig. 5 depicts wide notches at 7.15 GHz for three CMFSRRs of  $y = x = 2.35$  mm and  $l = 0.6$  mm placed equal distance  $d$  on the MMR. The notch width tends to reduce with increase of  $d$  due to weakening of EM coupling among the CMFSRR DGS units. Cascading two CMFSRR units generate less wider notch. Table 1 shows the comparison of notch

**Table 1.** BW: bandwidth.

$d$ (mm)	Two CMFSRR units BW (GHz)	Three CMFSRR units BW (GHz)
2.50	0.58	0.88
2.75	0.54	0.82
3.00	0.50	0.77

width for two and three equ-dimensional CMFSRR units placed equal distance  $d$  apart.

Similarly, multiple passband notches (dual, triple) are generated by cascading CMFSRR and CSRR DGS units of variable dimensions at some distance  $d$  on the MMR (inset of Fig. 6). Fig. 6 shows dual notches at 6.5 GHz and 9.2 GHz for CMFSRR ( $y_2 = x_2 = 2.35$  mm,  $l_2 = 1$  mm) and CSRR ( $y_1 = x_1 = 2.15$  mm), respectively, placed  $d = 3$  mm apart on the MMR. Triple notches at 6 GHz, 7.7 GHz and

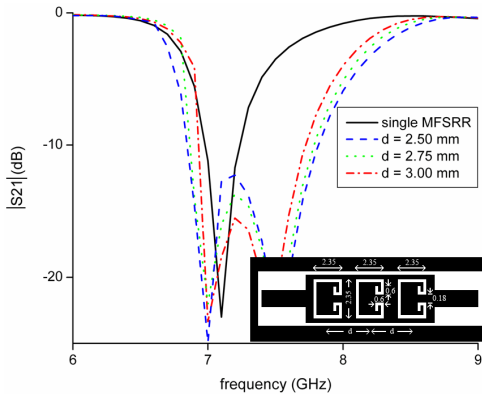


**Figure 5.** Widened notches centered at 7.15 GHz for three equ-dimensional CMFSRR units of  $y = x = 2.35$  mm and  $l = 0.6$  mm placed equal distance  $d = 3$  mm apart. Bandwidth of single CMFSRR unit is 0.21 GHz.

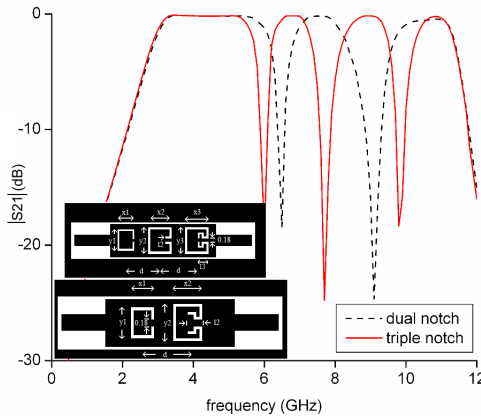


**Figure 6.** Dual and triple notches for CMFSRR and CSRR of variable dimensions placed equal distance  $d$  on the MMR.

9.8 GHz are obtained for CMFSRR ( $y_3 = x_3 = y_2 = x_2 = 2.35$  mm,  $l_3 = 1.25$  mm and  $l_2 = 0.4$  mm) and CSRR ( $y_1 = x_1 = 1.8$  mm), respectively, placed equal distance  $d = 3$  mm apart on the MMR. The dual and triple notch positions can be varied by varying the dimensions of the CMFSRR/CSRR DGS units.

## 2.2. Suppressed Stopband

MMR based filters have disadvantage of narrow upper stopband due to generation of higher order harmonics. To suppress these unwanted stopband harmonics, DEU-DGS units are implemented under the input and output feeding lines with open end alignment. Ting et al. in [9] showed that DEU-DGS unit generates dual finite attenuation poles at two different frequencies, with almost no change in characteristics of other frequencies. Positioning of these dual flexible poles is function of the DEU-DGS profile dimensions.

In DEU-DGS unit, when slots vertical length ( $y_1, y_2$ ) are kept fixed, on increasing the width of the horizontal section of the U slots ( $x_1$ ), both the attenuation poles are shifted to lower frequencies while both are pushed to higher frequencies when the width of the vertical sections of the U slots,  $x_2$  is increased. When widths ( $x_1, x_2$ ) of U slot are kept fixed, it is observed that the lower attenuation pole can be tuned by adjusting longer slot length  $y_2$  while higher pole can be tuned by adjusting shorter slot length  $y_1$ .

The original filter (without CMFSRR, CSRR and DEU-DGS units) possesses spurious stopband harmonics at 13.8 and 17.6 GHz, respectively. To suppress these harmonics the dimensional parameters of the DEU-DGS units are optimized to generate two attenuation poles at these frequencies without affecting the characteristics of other frequencies. The final optimized dimensions of the DEU-DGS obtained are:  $x_1 = 0.2$ ,  $x_2 = 0.5$ ,  $y_1 = 0.96$ ,  $y_2 = 2$  and  $y_3 = 1.6$  mm, respectively. When DEU-DGS of the above mentioned dimensions are applied to the original filter, the spurious harmonics at 13.8 GHz and 17.6 GHz are suppressed and stopband extended up to 17.8 GHz with attenuation greater than  $-24$  dB is obtained, as shown in Fig. 7(a).

Figure 7(b) displays spurious harmonics at 13.9 and 17.3 GHz, respectively, for the single notch structure (notch at 5.8 GHz, WLAN) shown in inset of Fig. 7(b). DEU-DGS of profile dimensions,  $x_1 = 0.2$ ,  $x_2 = 0.5$ ,  $y_1 = 0.96$ ,  $y_2 = 2$  and  $y_3 = 1.65$  mm, respectively, when applied to this structure suppresses these spurious harmonics and extends the stopband up to 18 GHz with attenuation greater than  $-18$  dB with no disturbance to the passband notch.

For the dual notch structure (inset of Fig. 7(c)), Fig. 7(c) shows undisturbed notches at 5.8 GHz (WLAN) and 8.15 GHz (X band)

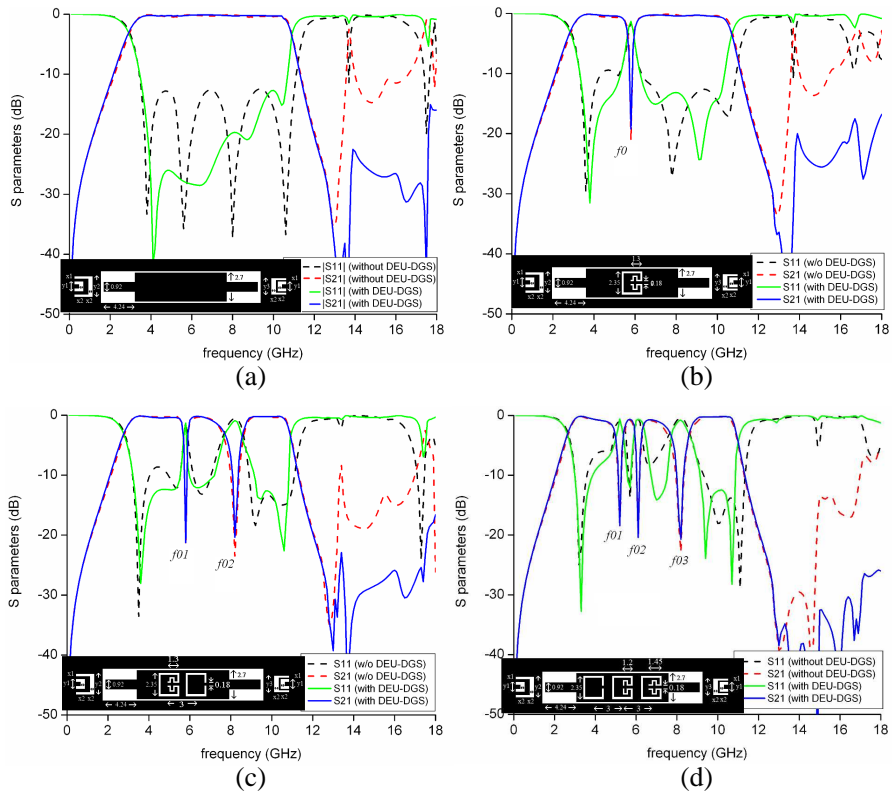


**Figure 7.** Frequency response for (a) original filter, (b) single notch, (c) dual notch and (d) the proposed triple notch structure with and without DEU-DGS units, respectively.

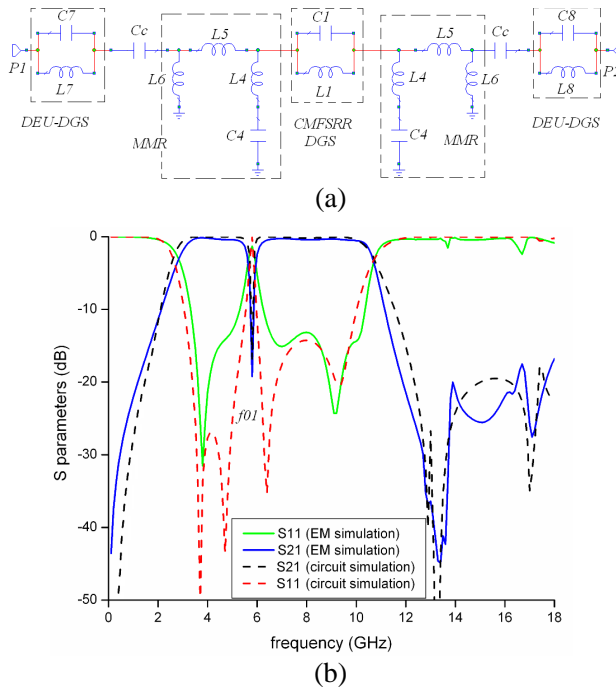
with stopband extended up to 17.6 GHz and attenuation greater than  $-20$  dB due to suppressed spurious harmonics at 13.5 GHz and 17.6 GHz when DEU-DGS of profile dimensions,  $x_1 = 0.2$ ,  $x_2 = 0.5$ ,  $y_1 = 0.96$ ,  $y_2 = 2.1$  and  $y_3 = 1.6$  mm, respectively, are applied to it.

Figure 7(d) displays the proposed triple notch structure with undisturbed notches at 5.2 GHz (WLAN), 6.1 GHz (C band) and 8.15 GHz (X band) when DEU-DGS of profile dimensions,  $x_1 = 0.2$ ,  $x_2 = 0.5$ ,  $y_1 = 0.96$ ,  $y_2 = 1.8$  and  $y_3 = 1.6$  mm respectively are applied to it. These DEU-DGS units generate dual attenuation poles at the spurious harmonics 15.6 GHz and 17.8 GHz which suppresses the stopband below  $-28$  dB and extends it up to 18 GHz.

### 3. EQUIVALENT CIRCUITS

Figure 8(a) displays the approximate equivalent circuit for the single notch structure. The passband width of the UWB filter is controlled by MMR profile dimensions, which in turn is function of inductances ( $L_4$ ,  $L_5$  and  $L_6$ ) and capacitance ( $C_4$ ). The parallel resonant circuits at either ends ( $L_7, C_7$  and  $L_8, C_8$ ) are the approximate equivalent of the DEU-DGS units. These DEU-DGS units are coupled to the MMR via the coupling capacitor  $C_c$ . The resonant circuit ( $L_1, C_1$ ) generates the passband notch at  $f_0 = 1/2\pi\sqrt{L_1C_1}$ . For the single notch structure with  $f_0$  at 5.8 GHz and stopband extended up to 18 GHz, the optimized circuit parameters obtained are  $L_1 = 0.114$  nH,  $L_4 = 1.92$  nH,  $L_5 = 1.16$  nH,  $L_6 = 4.32$  nH,  $L_7 = 0.0789$  nH,  $L_8 = 0.0489$  nH,  $C_c = 0.69$  pF,  $C_1 = 6.63$  pF,  $C_4 = 0.075$  pF,  $C_7 = 1.918$  pF,  $C_8 = 1.782$  pF. Fig. 8(b) represents the comparative frequency characteristics of the single notch filter for full wave EM and circuit simulation.

The equivalent circuit model of the multi notch structure consists of resonant circuits coupled via T-network (Fig. 9(a)) whose



**Figure 8.** (a) Approximate equivalent circuit for single notch structure. (b) Comparative  $S$  parameter EM and circuit simulation for single notch structure.

parameters ( $L_s$  and  $C_p$ ) are evaluated from [12] as:

$$C_{pi} = 1/(2\pi f_T X_{i,i+1}) \quad i = 1, 2$$

$$L_{si} = (X_{ii} - X_{21})/2\pi f_T + Li/((f_T/f_{0i})^2 - 1) \quad i = 1, 2, 3, 4.$$

where  $f_T$  is the transit frequency between resonant notch frequencies  $f_{oi}$ , and  $X$  is the imaginary part of  $Z$  parameter at the transit frequency  $f_T$ . For the dual notch structure with notch frequencies at  $f_{01} = 5.8$  GHz and  $f_{02} = 8.15$  GHz, the extracted optimized circuit parameters are:  $L_1 = 0.114$  nH,  $L_2 = 0.2063$  nH,  $L_4 = 1.92$  nH,  $L_5 = 1.16$  nH,  $L_6 = 4.32$  nH,  $L_7 = 0.0789$  nH,  $L_8 = 0.0489$  nH,  $L_{s1} = 0.979$  nH,  $L_{s2} = -0.858$  nH,  $C_c = 0.69$  pF,  $C_1 = 6.63$  pF,  $C_2 = 1.85$  pF,  $C_4 = 0.075$  pF,  $C_7 = 1.918$  pF,  $C_8 = 1.702$  pF,  $C_{p1} = 0.0133$  pF. The negative value of inductance  $L_{s2}$  is acceptable for circuit modeling as the case coincides with a lumped-element inverter possessing negative elements in which adjacent reactance components in the circuit physically absorb the negative elements [12]. The comparative frequency characteristics of the dual notch filter for full wave EM and circuit simulation is as shown in Fig. 9(b).

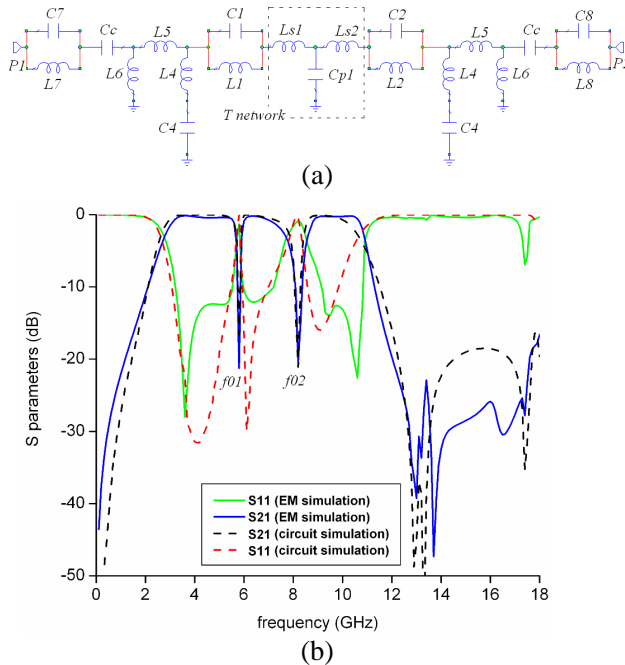


**Figure 9.** (a) Approximate equivalent circuit for dual notch structure. (b) Comparative  $S$  parameter EM and circuit simulation for dual notch structure.

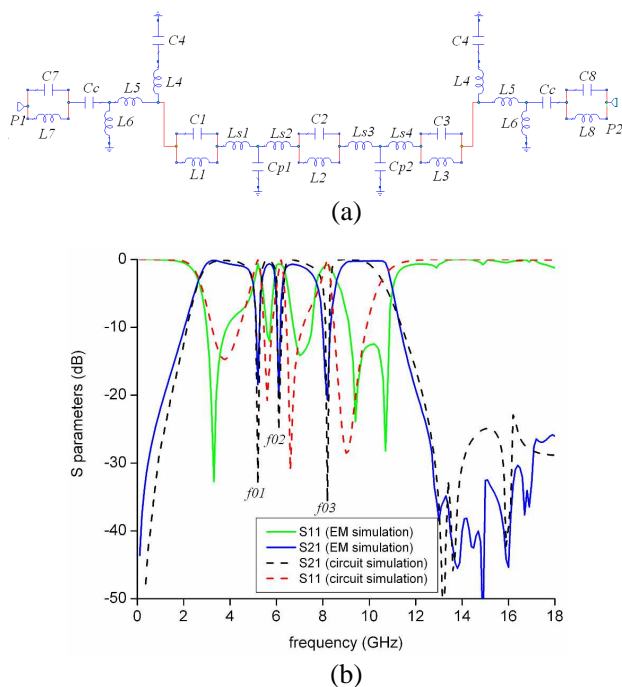


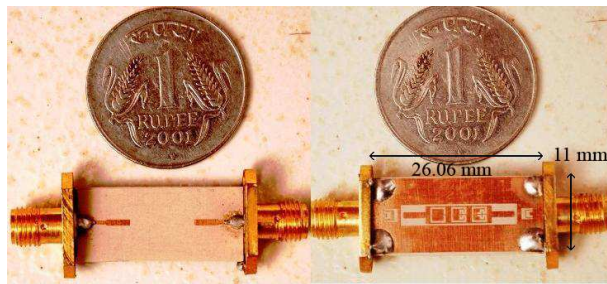
**Figure 10.** (a) Approximate equivalent circuit for triple notch structure. (b) Comparative  $S$  parameter EM and circuit simulation for triple notch structure.

The circuit parameters extracted for the proposed triple notch structure, shown in Fig. 10(a), with  $f_{01} = 5.2$  GHz,  $f_{02} = 6.1$  GHz and  $f_{03} = 8.15$  GHz are:  $L_1 = 0.412$  nH,  $L_2 = 0.207$  nH,  $L_3 = 0.206$  nH,  $L_4 = 2$  nH,  $L_5 = 1.51$  nH,  $L_6 = 4.32$  nH,  $L_7 = 0.0408$  nH,  $L_8 = 0.0678$  nH,  $L_{s1} = 0.989$  nH,  $L_{s2} = -0.822$  nH,  $L_{s3} = 0.955$  nH,  $L_{s4} = -0.822$  nH,  $C_c = 0.69$  pF,  $C_1 = 2.274$  pF,  $C_2 = 3.18$  pF,  $C_3 = 0.206$  pF,  $C_4 = 0.06805$  pF,  $C_7 = 2.448$  pF,  $C_8 = 2.15$  pF,  $C_{p1} = 0.00904$  pF,  $C_{p2} = 0.00648$  pF. Fig. 10(b) displays the comparative frequency characteristics of the proposed triple notch structure for full wave EM and circuit simulation.

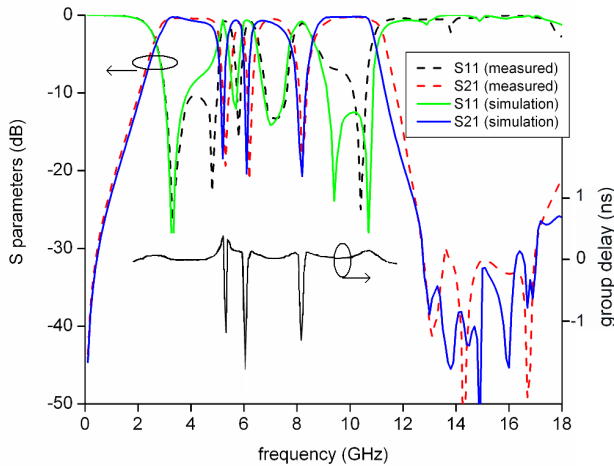
#### 4. RESULTS AND DISCUSSION

Figure 11(a) shows the proposed filter fabricated on RT Duroid 6010 of dielectric constant 10.8 and height 0.635 mm. The structure is measured using Agilent vector network analyzer N5230A and the

measured response is compared with EM simulation in Fig. 11(b). The passband (3 dB) observed is from 2.6–11.3 GHz while the upper-stopband extends up to 18 GHz with attenuation greater than 23 dB. The maximum insertion loss observed in the passband is 0.42 dB before the first notch, 0.95 dB between first and second notch, 0.78 dB between second and third notch and 0.48 dB after the third notch. High selectivity notched bands with 3 dB fractional bandwidth of 4.35%, 3.87% and 6.64% respectively, and attenuation greater than 18 dB at the centre notch frequency is observed. The group delay measured is  $< 0.34$  ns in the passband except at the notches. The discrepancy between measurements and simulations are mainly due to the fabrication error, finite substrate and reflection from connectors.



(a)



(b)

**Figure 11.** (a) Fabricated filter. (b) Comparative measured and simulated  $S$  parameters and group delay.

The overall size of the proposed filter is  $26.06 \text{ mm} \times 11 \text{ mm}$ . The above features make this UWB-BPF a better accessory than those reported in Table 2 [5–8].

**Table 2.** Comparison with some reported UWB filters with multiple notched bands.

Ref.	Dual notch/ frequency (GHz)/ Attenuation (dB)	Triple notch/ frequency (GHz)/ Attenuation (dB)
[5]	4.3 and 8/20	–
[6]	5.85 and 8/ > 15	–
[7]	5.2 and 5.8/ > 14	–
[8]	–	5.25, 5.85 and 8/ > 10
This work	Controllable/> 15	5.2, 6.1 and 8.15/ > 18
Ref.	Stopband width (GHz)/ depth (dB)	Overall Size (mm × mm)
[5]	Up to 14/ > 15	$23.6 \times 2.7$
[6]	Up to 12.7/ > 15	$34 \times 20$
[7]	Up to 13/ > 18	$32 \times 20$
[8]	Up to 20 / 15	$30.6 \times 20$
This work	Up to 18/ > 27	$26.06 \times 11$

It can be inferred from Table 2 that dual notched band UWB filters with very narrow stopband are reported in [5–7]. An UWB filter with triple notched band and simultaneously extended stopband is reported in [8], but it possesses the drawback of very low stopband attenuation depth (15 dB). Our structure on the other hand is capable of generating single and multiple controllable notches with simultaneously extended stopband (> 20 dB) in each case. The proposed structure size is much smaller compared to [6–8]. Our design provides the user with design flexibility and degree of freedom to eliminate single and/or multiple interferences with much improved isolation. An UWB filter with notch embedded function, improved isolation and miniaturized dimension is need of modern wireless communication system and our structure meets that requirement.

## 5. CONCLUSIONS

Application based UWB-BPF with triple notches at WLAN (5.2 GHz), C band (6.1 GHz) and X band (8.15 GHz) with simultaneously suppressed stopband (up to 18 GHz) and flat group delay ( $< 0.34$  ns in the passband) is proposed. The triple notches are implemented by cascading CMFSRR and CSRR DGS units in the MMR of the proposed structure while DEU-DGS units using their dual attenuation poles provide the suppressed stopband. The filter incorporates features of eliminating single and/or multiple interferences with improved isolation. The proposed structure exhibits better performance and compact size which makes it a useful candidate for use in present day UWB systems.

## REFERENCES

1. Wang, H. and L. Zhu, "Ultra-wideband bandpass filter using back-to-back microstrip-to-CPW transition structure," *Electronics Letters*, Vol. 41, No. 24, Nov. 24, 2005.
2. Li, K., D. Kurita, and T. Matsui, "An ultra-wideband bandpass filter using broadside-coupled microstrip-coplanar waveguide structure," *IEEE MTT-S Int. Dig.*, 675–678, Jun. 2005.
3. Kuo, T. N., S. C. Lin, and C. H. Chen, "Compact ultra-wideband bandpass filters using composite microstrip-coplanar-waveguide structure," *IEEE Trans. Microw. Theory Tech.*, Vol. 54, No. 10, 3772–3778, Oct. 2006.
4. An, J., G. M. Wang, W. D. Zeng, and L. X. Ma, "UWB filter using defected ground structure of von koch fractal shape slot," *Progress In Electromagnetics Research Letters*, Vol. 6, 61–66, 2009.
5. Song, K. and Q. Xue, "Compact ultra-wideband (UWB) bandpass filters with multiple notched bands," *IEEE Microwave and Wireless Component Letters*, Vol. 20, No. 8, 447–449, Aug. 2010.
6. Feng, W., Q. Y. Wu, X. W. Shi, and L. Chen, "Compact UWB bandpass filters with dual notched bands based on SCRLH resonator," *IEEE Microwave and Wireless Component Letters*, Vol. 21, No. 1, 28–30, Jan. 2011.
7. Liu, B.-W., Y.-Z. Yin, Y. Yang, S.-H. Jing, and A.-F. Sun, "Compact UWB bandpass filter with two notched bands based on electromagnetic bandgap structures," *Electronics Letters*, Vol. 47, No. 13, Jun. 23, 2011.
8. Feng, W., W. T. Li, X. W. Shi, and Q. L. Huang, "Compact UWB bandpass filters with triple-notched bands using triple mode

- stepped impedance resonator,” *IEEE Microwave and Wireless Component Letters*, Vol. 22, No. 10, 512–514, Oct. 2012.
9. Ting, S. W., K. W. Tam, and R. P. Martins, “Miniaturized microstrip lowpass filter with wide stopband using double equilateral U-shaped defected ground structure,” *IEEE Microwave and Wireless Component Letters*, Vol. 16, No. 5, 240–242, May 2006.
  10. Zeland Software Inc., *IE3D 14.0*, 2008.
  11. Zhu, L., R. Li, and S. Sun, *Microwave Bandpass Filter for Wideband Communications*, Wiley, 2012.
  12. Hong, S.-J. and B. M. Karyamapudi, “A general circuit model for defected ground structures in planar transmission lines,” *IEEE Microwave and Wireless Component Letters*, Vol. 15, No. 10, 706–708, Oct. 2005.